BRAIN
A JOURNAL OF NEUROLOGY

Longitudinal progression of Alzheimer's-like patterns of atrophy in normal older adults: the SPARE-AD index

Christos Davatzikos,[1] Feng Xu,[1] Yang An,[2] Yong Fan[1] and Susan M. Resnick[2]

1 Section of Biomedical Image Analysis, Department of Radiology, University of Pennsylvania, PA, USA
2 Laboratory of Personality and Cognition, National Institute on Ageing, Baltimore, Maryland, USA

Correspondence to: Prof. Christos Davatzikos,
Department of Radiology,
University of Pennsylvania,
3600 Market Street,
Suite 380, Philadelphia,
PA 19104,
USA
E-mail: christos@rad.upenn.edu

A challenge in developing informative neuroimaging biomarkers for early diagnosis of Alzheimer's disease is the need to identify biomarkers that are evident before the onset of clinical symptoms, and which have sufficient sensitivity and specificity on an individual patient basis. Recent literature suggests that spatial patterns of brain atrophy discriminate amongst Alzheimer's disease, mild cognitive impairment (MCI) and cognitively normal (CN) older adults with high accuracy on an individual basis, thereby offering promise that subtle brain changes can be detected during prodromal Alzheimer's disease stages. Here, we investigate whether these spatial patterns of brain atrophy can be detected in CN and MCI individuals and whether they are associated with cognitive decline. Images from the Alzheimer's Disease Neuroimaging Initiative (ADNI) were used to construct a pattern classifier that recognizes spatial patterns of brain atrophy which best distinguish Alzheimer's disease patients from CN on an individual person basis. This classifier was subsequently applied to longitudinal magnetic resonance imaging scans of CN and MCI participants in the Baltimore Longitudinal Study of Aging (BLSA) neuroimaging study. The degree to which Alzheimer's disease-like patterns were present in CN and MCI subjects was evaluated longitudinally in relation to cognitive performance. The oldest BLSA CN individuals showed progressively increasing Alzheimer's disease-like patterns of atrophy, and individuals with these patterns had reduced cognitive performance. MCI was associated with steeper longitudinal increases of Alzheimer's disease-like patterns of atrophy, which separated them from CN (receiver operating characteristic area under the curve equal to 0.89). Our results suggest that imaging-based spatial patterns of brain atrophy of Alzheimer's disease, evaluated with sophisticated pattern analysis and recognition methods, may be useful in discriminating among CN individuals who are likely to be stable versus those who will show cognitive decline. Future prospective studies will elucidate the temporal dynamics of spatial atrophy patterns and the emergence of clinical symptoms.

Introduction

Alzheimer's disease poses significant medical, social and socio-economic challenges, as it is the most common dementia, with incidence rates doubling every 5 years after the age of 65. Although there are currently no disease-modifying treatments, many potential treatments are being tested, some of which may have significant side-effects. Thus, it is critical to identify biomarkers that identify early stages of the disease and facilitate effective and well-targeted treatment before significant neuronal damage.

Neuroimaging measures have been playing a central role in the search for biomarkers of Alzheimer's disease that can be used for early diagnosis and monitoring of disease progression and response to therapy. Recent studies have focused on individuals with mild cognitive impairment (MCI), who have higher rates of conversion to Alzheimer's disease (as high as 15% per year) than cognitively normal (CN) individuals (Petersen et al., 1999). Many investigators consider MCI to be early Alzheimer's disease, as it has been shown that many MCI individuals have similar patterns of atrophy and β-amyloid deposition as Alzheimer's disease patients (Chetelat et al., 2002; Karas et al., 2004; Klunk et al., 2006; Ziolko et al., 2006; Rowe et al., 2007; Fan et al., 2008), albeit some MCI individuals remain clinically stable over time and, consistently, some also present normal structural brain profiles (Fan et al., 2008). Given the high rates of conversion from MCI to Alzheimer's disease and the abundant neuropathology already evident in MCI post-mortem (Mufson et al., 1999; Scheff et al., 2006), greater emphasis should be placed on identifying those CN individuals who present evolving Alzheimer's disease-like patterns of brain atrophy and might be relatively more likely to progress to MCI and Alzheimer's disease. Identification of such individuals at a very early stage before the onset of clinical symptoms may lead to more effective intervention of pharmacological treatments for Alzheimer's disease as these become available.

Several longitudinal studies of normal ageing have measured brain changes through regions of interest (ROI) and voxel-based analysis (Golomb et al., 1993; Convit et al., 1997; Mueller et al., 1998; Convit et al., 2000; Resnick et al., 2001; Sullivan et al., 2002; Resnick et al., 2003) and have increased our understanding about how different brain regions change in normal ageing populations. Although total brain or regions of interest volumes may be reduced with ageing and Alzheimer's disease, their inter-individual variations and overlap across populations render them insufficient diagnostic tools for individuals, especially at early disease stages. The development of high-dimensional pattern classification methods in recent years (Lao et al., 2004; Fan et al., 2007b; Kloppel et al., 2008; Vemuri et al., 2008) offers the potential to obtain highly sensitive and specific neuroimaging biomarkers from individuals, rather than groups, which has great importance for early diagnosis and for individual patient management. These methods use sophisticated pattern analysis algorithms that are trained to identify patterns of normal or abnormal structure and function (Davatzikos et al., 2005a), which are used for classification at the individual level. We have shown previously that spatial patterns of brain atrophy discriminate between CN and Alzheimer's disease with high accuracy [areas under the receiver operating characteristic (ROC) curve: 0.965] (Fan et al., 2008).

Here, we investigate whether these spatial patterns of brain atrophy can distinguish among CN individuals and whether these patterns are associated with cognitive decline. The current study is the first, to our knowledge, to utilize high-dimensional pattern classification to evaluate the progression of abnormal patterns of brain atrophy in a prospectively followed CN cohort of older adults. We first train the classifier to recognize spatial patterns of brain atrophy that distinguish Alzheimer's disease from CN individuals in the Alzheimer's Disease Neuroimaging Initiative (ADNI) cohort. The classifier produces an algorithm for determination of a quantitative value for each individual, which we refer to as the SPARE-AD index (Spatial Pattern of Abnormality for Recognition of Early Alzheimer's disease). More positive SPARE-AD implies a more Alzheimer's disease-like pattern of brain atrophy, and more negative SPARE-AD implies a more normal pattern of brain morphology. The ADNI classifier is then applied to MRI scans of CN and MCI participants from the Baltimore Longitudinal Study of Ageing (BLSA) to determine the presence and longitudinal progression of these patterns via longitudinal progression of the SPARE-AD index. Finally, the cognitive performance of CN individuals displaying abnormal patterns of brain atrophy is compared to CN individuals displaying normal brain structure. Since the BLSA is a prospective study, it provides the opportunity to detect very early stages of Alzheimer's disease.

Material and Methods

BLSA participants

The BLSA is a prospective longitudinal study of ageing. Its neuroimaging component, currently in its 14th year, has followed 158 individuals (aged 55–85 years at enrolment) with annual or semi-annual imaging and clinical evaluations. The neuroimaging substudy of the BLSA is described in detail in (Resnick et al., 2000, 2003). Exclusionary criteria at initial evaluation were CNS disease (epilepsy, stroke, bipolar illness, previous diagnosis of dementia), severe cardiovascular disease (myocardial infarction, coronary artery disease requiring angioplasty or bypass surgery), severe pulmonary disease or metastatic cancer. The current study used longitudinal data from 109 BLSA participants that have remained CN up to September 2007. It also used longitudinal data from 15 individuals that were diagnosed with MCI over the course of the BLSA neuroimaging study. A diagnosis of MCI was assigned by consensus conference if a participant had deficits in either a single cognitive domain (usually memory) or had more than one cognitive deficit but did not have functional loss in activities of daily living. Participants were evaluated at the consensus conference if their Blessed Information Memory Concentration (Blessed et al., 1968) score was greater than three or if their informant or subject Clinical Dementia Rating (CDR) (Morris, 1997) score was 0.5 or above. The demographic characteristics of the BLSA participants in this study are shown in Table 1.

The BLSA and neuroimaging studies are approved by the local institutional review boards, and all participants gave written informed consent prior to each assessment.

Table 1 Characteristics of the BLSA participants in the current study

Group	MCI	CN
No. of subjects	15	109
Sex: no. of males	10	60
Baseline age, mean (SD)	77.0 (7.2)	68.8 (7.7)
Age at last visit, mean (SD)	82.9 (7.1)	75.6 (8.1)
MMSE at first visit, mean (SD)	27.2 (2.5)	28.9 (1.3)
MMSE at last visit, mean (SD)	25.4 (3.0)	28.8 (1.2)

ADNI participants

The ADNI is described in www.adni-info.org. The goal of ADNI is to recruit 800 adults, ages 55–90 years, approximately 200 CN older individuals to be followed for 3 years, 400 people with MCI to be followed for 3 years and 200 people with early Alzheimer's disease to be followed for 2 years. For up-to-date information see www.adni-info.org. The data of all ADNI participants used in the current study have been described previously (Fan *et al.*, 2008). Briefly, MRI scans from 66 CN individuals (mean age ± SD 75.18 ± 5.39), and 56 Alzheimer's disease patients (77.40 ± 7.02) were analysed and used to construct a classifier to discriminate between CN and Alzheimer's disease. The MMSE scores (mean ± SD) of the CN and Alzheimer's disease groups at baseline were 29.1 ± 1.0, and 23.1 ± 1.8, respectively. The groups were relatively well balanced in terms of sex (50%, 57% women in CN and Alzheimer's disease groups, respectively).

Image acquisition

We used T_1-weighted MR images to measure regional patterns of brain atrophy. The image acquisition parameters have been described in (Resnick *et al.*, 2001) for BLSA, and in www.adni-info.org for ADNI. Briefly, the BLSA protocol included an axial T_1-weighted volumetric spoiled gradient recalled (SPGR) series (axial acquisition, TR = 35 ms, TE = 5 ms, flip angle = 45°, voxel dimensions of 0.94 × 0.94 × 1.5 mm slice thickness). The ADNI protocol included a sagittal volumetric 3D MPRAGE with 1.25 × 1.25 mm in-plane spatial resolution and 1.2-mm thick sagittal slices (8° flip angle). TR and TE values of the ADNI protocol were somewhat variable, but the target values were TE ∼3.9 ms and TR ∼8.9 ms.

Image analysis

Images were first pre-processed according to previously validated and published techniques (Goldszal *et al.*, 1998). The pre-processing steps included: (i) alignment to the AC-PC plane; (ii) removal of extra-cranial material (skull-stripping); (iii) tissue segmentation into grey matter, white matter and cerebrospinal fluid (CSF) (Pham and Prince, 1999); (iv) high-dimensional image warping (Shen and Davatzikos, 2002) to a standardized coordinate system, a brain atlas (template) that was aligned with the Montreal Neurologic Institute coordinate space (Kabani *et al.*, 1998); and (v) formation of regional volumetric maps, named RAVENS maps (Goldszal *et al.*, 1998; Davatzikos *et al.*, 2001; Shen and Davatzikos, 2003), using tissue preserving image warping (Goldszal *et al.*, 1998). RAVENS map intensity values quantify the regional distribution of grey matter, white matter and CSF, with one RAVENS map for each tissue type. In particular, RAVENS values in the template's (stereotaxic) space are directly proportional to the volume of the respective structures in the original brain scan. Therefore, regional volumetric measurements and comparisons are performed via measurements and comparisons of the respective RAVENS maps. For example, patterns of grey matter atrophy in the temporal lobe are quantified by patterns of RAVENS decrease in the temporal lobe in the stereotaxic space.

The RAVENS approach has been extensively validated (Goldszal *et al.*, 1998; Davatzikos *et al.*, 2001) and applied to a variety of studies (Resnick *et al.*, 2000, 2001, 2003, 2004; Kim *et al.*, 2003; Beresford *et al.*, 2006*a, b*; Gur *et al.*, 2006; Stewart *et al.*, 2006; Driscoll *et al.*, 2007). It bears similarities with the 'optimized voxel based morphometry (VBM)' approach (Good *et al.*, 2002), except it uses a highly conforming high-dimensional image warping algorithm that captures finer structural details.

High-dimensional classification: the SPARE-AD index as a biomarker for Alzheimer's disease

We applied a high-dimensional pattern classification approach, which we have published and applied in a number of neuroimaging studies (Lao *et al.*, 2004; Davatzikos *et al.*, 2005*b*; Fan *et al.*, 2005, 2007*a*, 2008). This approach considers all brain regions jointly and identifies a minimal set of regions whose volumes jointly maximally differentiate between CN and Alzheimer's disease on an individual scan basis. As described in the Introduction section, the pattern classification method provides a SPARE-AD index; more positive SPARE-AD implies more Alzheimer's disease-like brain structure, and more negative SPARE-AD implies more normal structure. The pattern classifier determined the spatial patterns of brain atrophy that best distinguished Alzheimer's disease patients from CN on an individual person basis using the ADNI sample; as anticipated, these patterns tended to reflect regional atrophy in the temporal lobe, posterior cingulate and other areas known to be affected in Alzheimer's disease (Fan *et al.*, 2008).

We first evaluated the frequency of more Alzheimer's disease-like SPARE-AD values in CN individuals for different age groups, and compared RAVENS maps of CN individuals in the upper quartile versus the remaining 75% of SPARE-AD scores. To illustrate the network of regions contributing to SPARE-AD differences between CN in the top quartile versus lower quartiles of SPARE-AD, group comparisons were performed via voxel-based statistical analysis software (http://www.fil.ion.ucl.ac.uk/spm/software/spm5) of respective RAVENS maps that were normalized by an approximation to the total intra-cranial volume (ICV), so that spatial patterns of atrophy are examined without the confounding effect of head size. This approximation to ICV was obtained by summing the volumes of grey matter, white matter, ventricular, as well as the CSF within the sulci of the cortex that are contained within the outer brain boundary defined by the skull stripping algorithm. The approximation to ICV, which correlates ($r = 0.93$) with the more traditional approach to definition of ICV, was employed in this analysis for consistency with the approach used in the development of the ADNI classifier. RAVENS maps were smoothed prior to statistical analysis using 8 mm full-width at half-maximum smoothing kernel.

Next, we evaluated the longitudinal progression of SPARE-AD in normals and in MCI by applying the classifier developed on the ADNI sample to all longitudinal MRI scans of the BLSA CN and MCI individuals, thereby allowing us to follow the evolution of the SPARE-AD index with increasing age. Mixed-effects models were used to estimate individual SPARE-AD rates of change, defined as annual changes in SPARE-AD scores. Mixed models with cognitive status

(MCI versus CN) as a predictor were used to test the difference in rates for MCI versus CN.

Cognitive evaluations and associations with SPARE-AD

To determine the relationship between SPARE-AD progression and cognitive performance, we examined the SPARE-AD index values and rates of change in the SPARE-AD index in relation to performance on tests of mental status and memory. From the battery of neuropsychological tests administered to participants in conjunction with each imaging evaluation, we selected four measures for analysis. The four measures used in the current analyses were the total score from the Mini-Mental State Exam (MMSE) (Folstein et al., 1975) to assess mental status, the immediate free recall score (sum of five immediate recall trials) and the long-delay free recall score on the California Verbal Learning Test (CVLT) (Delis et al., 1987) to assess verbal learning and immediate and delayed recall, and the total number of errors from the Benton Visual Retention Test (BVRT) (Benton, 1974) to assess short-term visual memory. We focused on these measures because changes in new learning and recall are among the earliest cognitive changes detected during the prodromal phase of Alzheimer's disease (Grober et al., 2008). To examine relationships between SPARE-AD and cognitive performance, CN individuals in the highest quartile of SPARE-AD index values (most Alzheimer's disease-like) were compared with the remaining sample. Relationships between SPARE-AD and the four measures of cognitive performance were examined by t-tests for unadjusted analyses and by analysis of covariance for analyses adjusted for age and sex.

Results

Prevalence of Alzheimer's disease-like SPARE-AD in CN

Table 2 summarizes the SPARE-AD index values as a function of age decade for the CN BLSA participants, including all 818 scans of the 109 CN. In particular, in Table 2 we have summarized the age distribution of positive SPARE-AD scores, as well as of the top 25% SPARE-AD scores. We report each scan individually (numbers not in parentheses) and numbers of subjects (numbers in parentheses) that fall in each age group. For the latter, we used

average SPARE-AD and average age. Percentages are reported relative to the number of scans (subjects) in the respective age range. Overall, CN below the age of 80 years had negative SPARE-AD. However, Alzheimer's disease-like scores were more frequent in older individuals, even though these individuals had normal cognition by clinical consensus criteria. Figure 1 plots the mean SPARE-AD score of each of the 109 CN individuals against mean age over each participant's follow-up period. The Pearson correlation between mean SPARE-AD score and mean age is 0.43 ($P < 0.0001$), which is highly significant. Although the quadratic term does not reach significance, a Box–Cox transformation (with $\lambda = -3$) provides the best fit to the data ($r = 0.44$; $P < 0.001$) and indicates the presence of a nonlinear association.

Spatial patterns of atrophy

In order to visually investigate the spatial pattern of regional volumetric differences between the CN with the highest SPARE-AD scores (the top quartile, referred to as CN_high) and the CN with SPARE-AD scores in the lower 75% (referred to as CN_low), we performed voxel-wise analysis of the grey matter and white matter RAVENS maps. Figure 2 shows regions where the CN_high
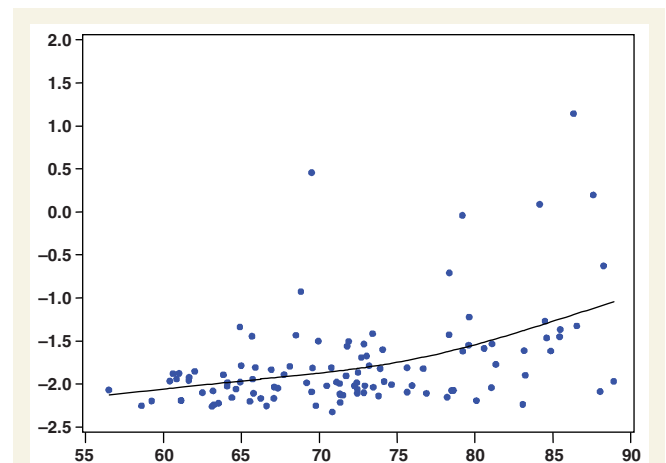

Figure 1 Mean SPARE-AD scores of each of the 109 CN individuals plotted against mean age over their follow-up period.

Table 2 Statistics of the SPARE-AD for the total of 818 scans of all 109 CN

Age (years)	50–59	60–69	70–79	80–89	⩾ 90	Total
Total no. of scans (subjects)	27 (3)	304 (42)	329 (44)	146 (20)	12 (0)	818 (109)
SPARE-AD > 0						
No. of scans (subjects)	0 (0)	4 (1)	5 (0)	22 (3)	3 (0)	34 (4)
Percentage of scans (subjects)	0 (0)	1.32 (2.38)	1.52 (0)	15.07 (15)	25.00 (0)	4.16 (3.67)
SPARE-AD in upper quartiles						
Number of scans (subjects)	0 (0)	33 (6)	79 (10)	86 (11)	6 (0)	204 (27)
Percentage of scans (subjects)	0 (0)	10.9 (14.3)	24 (22.7)	58.9 (55)	50 (NaN)	24.9 (24.8%)

Numbers outside parentheses indicate results obtained by treating each scan as an individual measurement, and numbers in parentheses indicate results obtained by finding the average SPARE-AD and age of all scans of a given individual, and then using the average value as a single measurement of that individual. The total number of scans per group is shown at the top row; each subject has multiple scans, one per visit. The total number of subjects per group is shown at the top row in parentheses. Percentages were calculated relative to the total number of scans (subjects) in each age category.
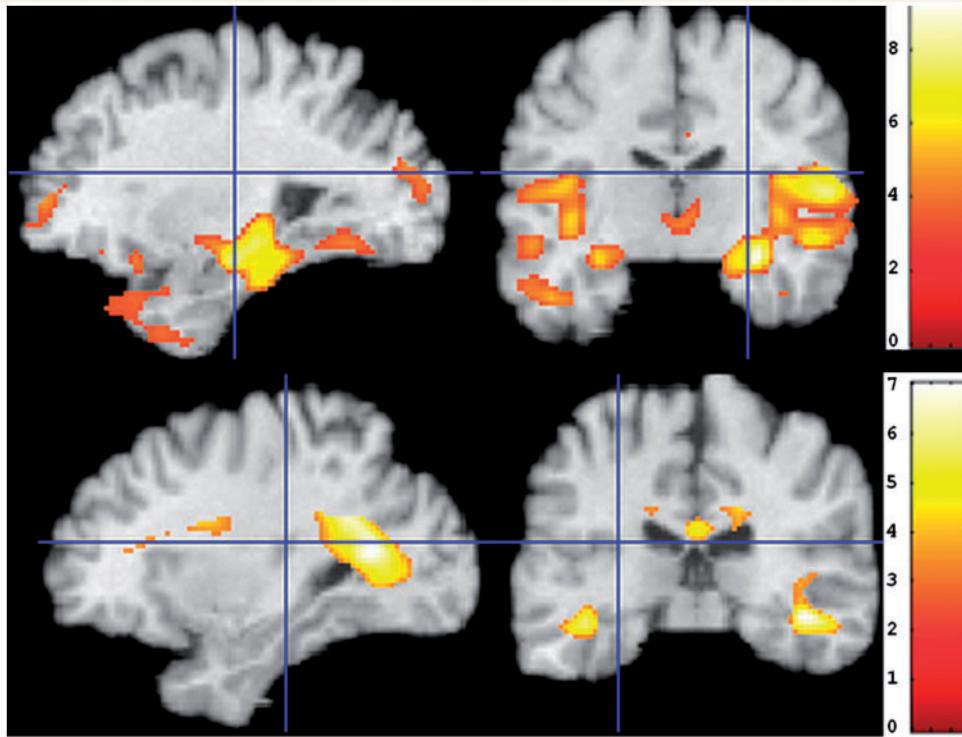
Figure 2 The *t*-statistic voxel-wise maps of RAVENS grey matter (top) and white matter (bottom) comparing the 75% of CN individuals with the lowest SPARE-AD scores (CN-like CN) minus those with the top 25% SPARE-AD (relatively more Alzheimer's disease-like CN). The images are in neurology convention, so left in the image is the left brain hemisphere.

showed less grey and white matter volumes, respectively, compared to the CN_low subjects. Significant decreases in tissue volumes in the more Alzheimer's disease-like CN were evident primarily in the temporal lobe. We note that the classifier used to derive the SPARE-AD score uses regions from the temporal lobe, the cingulate and the insula, as described in Fan (2008 #2464), because those are the regions that best discriminate between Alzheimer's disease and CN. Therefore, it is reasonable that the group differences, observed herein, are primarily located in these regions. Figure 2, therefore, should be interpreted as a visual representation the atrophy patterns that lead to the SPARE-AD scores described in our results.

Because regions of abnormal white matter on T_1 images appear dark and are typically segmented as grey matter, we also examined regions of grey matter that appeared to have greater volumes in the CN_high SPARE-AD group. The CN_high group appeared to have more grey matter tissue around the ventricles (Fig. 3, left), especially the posterior periventricular regions, which are white matter regions that tend to present small vessel pathology in older individuals.

Figure 3 Regions in which CN individuals with the top 25% (highest) SPARE-AD scores had significantly higher grey matter RAVENS maps than the bottom 75%, indicating increased periventricular abnormal white matter tissue that appears grey in T_1-weighted images and is segmented as grey matter. The image is in radiology convention: Top in the image is left hemisphere.

Longitudinal progression of SPARE-AD in CN

The rates of longitudinal progression of the SPARE-AD index of the 109 CN are shown in Fig. 4, as a function of mean age during each perso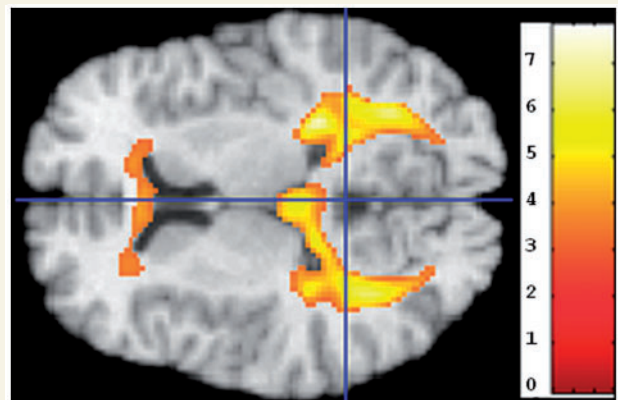n's follow-up period. Because the number of available follow-up scans varied considerably across individuals, mixed-effects regression was used to estimate all rates of change and shows significant increases in rates of SPARE-AD with age ($P<0.001$). For illustration, the rates are shown as a function of age, with a Pearson correlation between rates of SPARE-AD change and mean age of 0.45 ($P<.0001$), with a significant
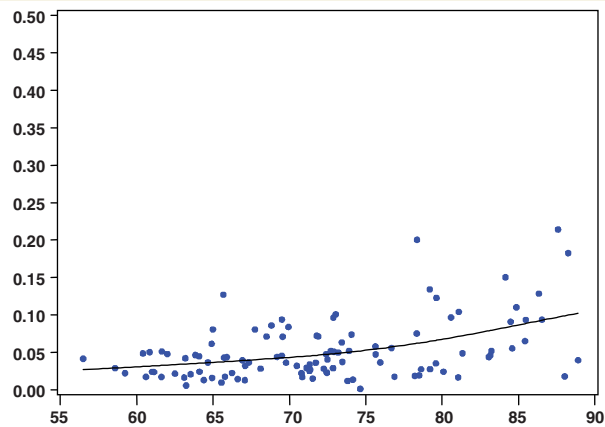
Figure 4 Rate of SPARE-AD change as a function of average age during follow-up period, for the 109 CN individuals.
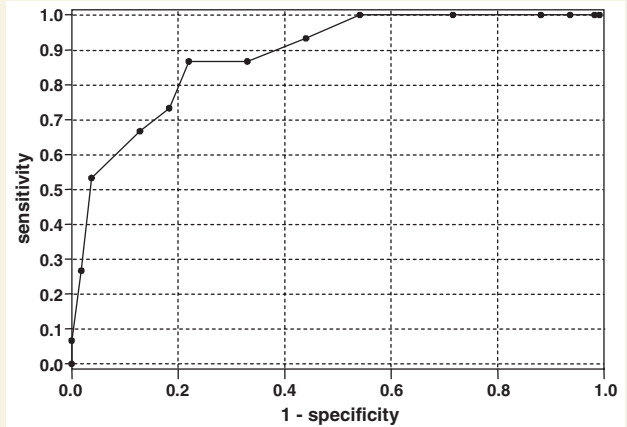

Figure 6 ROC curve of individual subject classification to CN or MCI, based on the rate of SPARE-AD change. AUC = 0.885.
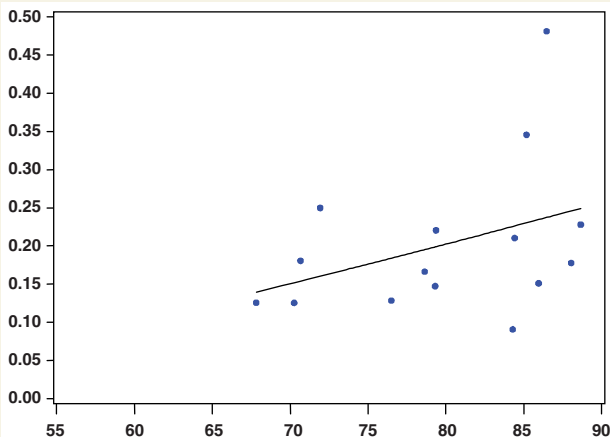

Figure 5 SPARE-AD annual change rates plotted against age for all MCI individuals.

quadratic effect ($P<0.05$). The increasing longitudinal rates of SPARE-AD change with age are consistent with the nonlinearly increasing SPARE-AD values with age shown in the cross-sectional analysis in Fig. 1.

Longitudinal rate of change of SPARE-AD in MCI

The rates of SPARE-AD change of the 15 participants who were diagnosed with MCI over the course of the study are plotted in Fig. 5 against the age of the participants. Most of these individuals showed relatively rapid increase of the SPARE-AD index, even though their SPARE-AD scores were largely in the negative range (only 14 of the 97 scans had positive scores consistent with their relatively mild stage of impairment). Mixed-effects models were used to compare rates of change in CN versus MCI. Rates of change were significantly greater in MCI compared with CN (estimate = 0.15, SE = 0.017, $P<0.0001$).

Separability of CN and MCI on an individual subject basis, based on rate of SPARE-AD change

For individual patient management, it is important to be able to determine whether the individual is likely to remain stable or convert to MCI. We constructed a ROC curve, by varying the threshold applied to the rate of SPARE-AD change and assigning individuals with rates of change higher than the threshold to MCI, and vice versa for CN. Figure 6 shows the ROC curve, which achieved an area under the curve (AUC) equal to 0.89.

Relationship between cognitive performance and SPARE-AD in CN

Cross-sectional analyses of the four cognitive measures (CVLT Sum of Immediate Free Recall, CVLT Delayed Free Recall and BVRT errors) in relation to SPARE-AD were performed using subgroups determined from the mean SPARE-AD, the SPARE-AD at the first imaging visit and the SPARE-AD at the last imaging visit. Cognitive performance between SPARE-AD groups was compared by t-test for unadjusted index values, and by analysis of covariance for SPARE-AD adjusted for age and sex. As shown in Table 3, using mean SPARE-AD and mean cognitive performance unadjusted for age and sex, both short and long-term verbal memory scores were significantly lower ($P<0.01$) in CN_high compared with CN_low groups. Using SPARE-AD groupings and cognitive scores from the first visit, MMSE in addition to CVLT performance was significantly lower ($P<0.01$) in the CN_high compared with CN_low groups. Cognitive performance did not differ between groups using data from the last follow-up, and only the results for the MMSE at the first visit remained significant after adjusting for age and sex.

We also divided individuals by the rate of SPARE-AD change, yielding a high versus low change group. Again, CN with high rates of SPARE-AD increase (the top 25% rate of SPARE-AD change values) showed significantly lower CVLT learning and

Table 3 *P*-values of cross-sectional differences in cognitive performance between the CN subjects with the top 25% of the SPARE-AD scores and the remaining 75%

	Mean scores	Mean scores adjusted (for sex and age)	First visit scores	First visit scores adjusted	Last visit scores	Last visit scores adjusted
CVLT List A Sum	0.0075	0.5155	0.0020	0.1797	0.3357	0.3754
CVLT Long Delay Free	0.0067	0.3150	0.0067	0.2674	0.1817	0.8458
BVRT Errors	0.0930	0.9728	0.3505	0.8944	0.5994	0.5592
MMSE	0.1719	0.9666	0.0092	0.0174	0.5203	0.8606

Column labels indicate the scores used in the analysis, e.g. 'mean scores' indicates the *P*-value is based on mean cognitive performance and mean SPARE-AD index over time. Covariates in adjusted comparisons are baseline age and sex.

Table 4 *P*-values of differences in cognitive performance between the CN individuals with high rates of SPARE-AD change and CN individuals with low rates of SPARE-AD change (remaining 75%)

	Mean cognitive score	Mean cognitive score adjusted	First visit cognitive score	First visit cognitive score adjusted	Last visit cognitive score	Last visit cognitive score adjusted
CVLT List A Sum	0.0295	0.4784	0.0250	0.3792	0.0190	0.2780
CVLT Long Delay Free	0.0448	0.5288	0.0455	0.4476	0.0066	0.1018
BVRT Errors	0.3987	0.4906	0.6139	0.6453	0.3302	0.9097
MMSE	0.2020	0.8316	0.3475	0.8306	0.0579	0.1901

Covariates in adjusted comparisons are baseline age and sex.

memory performance compared with CN with low rates of SPARE-AD change (Table 4). In addition, CN with high rates of SPARE-AD change had poorer performance on the MMSE, a measure of mental status, during the last visit. However, these findings were no longer significant after adjustment for age and sex.

Relationship between cognitive performance and SPARE-AD in MCI

In the group of 15 participants diagnosed as MCI over the course of the study, the individuals with positive SPARE-AD, as well as the ones with relatively higher rates of SPARE-AD change, showed relatively worse cognitive performance. We did not examine quartiles, due to the small sample size. Mixed-effects regression showed a significant association between the SPARE-AD index and MMSE scores of individuals diagnosed with MCI (estimate = −1.23, SE = 0.33, *P* < 0.001, Fig. 7).
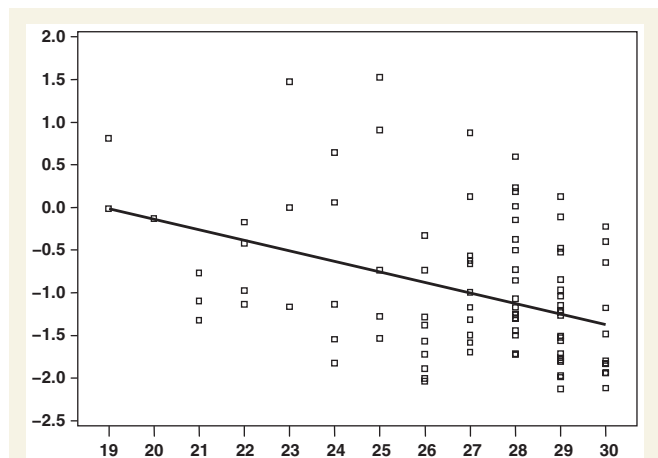

Figure 7 SPARE-AD index values (vertical axis) plotted against MMSE scores for all MCI individuals. The linear effect (*P* < 0.001) was determined using mixed-effects regression.

Discussion

A variety of neuroimaging studies have examined brain structure, as well as its longitudinal change, in CN samples and in MCI and Alzheimer's disease via group analyses. We introduced the use of support vector machine learning approaches for classification of CN and impaired individuals at an individual level, as opposed to investigating group differences (Lao *et al*., 2004; Davatzikos *et al*., 2008; Fan *et al*., 2007*b*). The potential of this approach for individual classification and diagnosis has been confirmed recently

by others (Duchesne *et al*., 2008; Kloppel *et al*., 2008; Vemuri *et al*., 2008). Our current study builds upon a computer-based pattern classification method constructed in Fan *et al*. (2008) to detect spatial patterns of brain atrophy that distinguish between Alzheimer's disease patients and CN on an individual basis. In this study, we applied the classification algorithm that distinguished between Alzheimer's disease patients and CN subjects in the ADNI to a different sample of CN and MCI subjects from the BLSA. This approach generates a CN-like (negative) and Alzheimer's disease-like (positive) SPARE-AD index of spatial

atrophy patterns. We examined the frequency and longitudinal progression of Alzheimer's disease-like spatial atrophy patterns in the BLSA cohort of CN elderly, as well as in relatively mild MCI individuals.

Our results indicate that although the vast majority of CN have negative SPARE-AD and remain relatively stable over time, the proportion of individuals showing more Alzheimer's disease-like, even positive, SPARE-AD increases with age. Comparisons of CN groups showing relatively higher SPARE-AD and CN individuals with relatively lower SPARE-AD revealed differences in spatial atrophy patterns consistent with the pattern of atrophy characteristic of Alzheimer's disease. A strength of this study is that we examined SPARE-AD patterns in CN individuals who have been followed prospectively and remained clinically normal during the study follow-up period. Despite the lack of clinically evident impairment, CN individuals in the upper quartile of SPARE-AD, compared with the remaining CN individuals, had significantly lower performance on tests of mental status and immediate and delayed verbal memory. Declines in verbal episodic memory are among the earliest cognitive changes preceding a diagnosis of dementia, by as much as an average of seven years when investigated within the context of a prospective study (Grober et al., 2008), and the most robust grey matter differences contributing to the SPARE-AD classifier involved temporal lobe structures, which are critical for maintenance of intact memory performance. Moreover, individuals with steeper increases in the rate of SPARE-AD had lower cognitive performance. The majority of associations between cognitive performance and SPARE-AD index did not hold after adjusting for age, indicating overlap in the factors mediating spatial atrophy change and cognitive change. This is not unexpected, since cognitive decline occurs in parallel with brain tissue loss in ageing populations, and age-adjustment may remove the relationship of interest. More sophisticated dynamic modeling of longitudinal data and statistical approaches which avoid age-adjustment in larger samples may be necessary to determine whether SPARE-AD has a robust association with cognitive performance.

Notably, cross-sectional relationships between the SPARE-AD index and cognitive scores were evident for the mean values and those at the first but not the last visit. The absence of associations for the last visits when participants are older is consistent with post-mortem findings that Alzheimer's disease neuropathology may show a different pattern in the oldest participants (Giannakopoulos et al., 1995). Future longitudinal follow-up of these individuals, half of which are also enrolled in the BLSA autopsy study, will further elucidate the predictive value of high SPARE-AD or high rate of SPARE-AD change for Alzheimer's disease neuropathology. However, our results indicate that the SPARE-AD index might potentially be an important early biomarker of Alzheimer's disease progression, even before symptoms come to clinical attention. The longitudinal stability of the SPARE-AD index in CN with more negative scores, as indicated by low rates of change, indicates that SPARE-AD might be a relatively objective tool, which will assist in the evaluation of structural phenotypes associated with Alzheimer's disease and aid in the discrimination of CN who are likely to remain stable versus those who are at greatest risk for memory impairment.

A much larger proportion of the MCI individuals showed high rates of SPARE-AD change, as expected. The MCI group also showed a relatively large and uniform spread in the range of ~0.1–0.5 per year, which indicates a rather rapid progression of Alzheimer's disease-like brain atrophy. This agrees with the well documented finding that MCI individuals are quite heterogeneous, and that some will convert to Alzheimer's disease in the following years whereas others will remain stable for a long period. As these MCI individuals were identified within the context of prospective BLSA follow-ups rather than referrals to memory clinics, they are initially studied during very early stages of impairment and have relatively mild MCI. This is in agreement with the fact that most MCIs had negative SPARE-AD albeit many had high rates of change, indicating that rate of change may be a stronger predictor of conversion to Alzheimer's disease. Further follow up of the entire BLSA cohort will allow us to evaluate the predictive value of the SPARE-AD and its rate of change in MCI converters to Alzheimer's disease.

Our ability to distinguish between MCI and CN using a single value, namely the rate of SPARE-AD change, is very promising. In addition, CN individuals with high rates of SPARE-AD change showed lower cognitive performance; thus, CN individuals that were 'misclassified' as MCI based on SPARE-AD index might actually develop MCI in the near future. However, we did not find any particular relationship between the exact year of conversion and the SPARE-AD. Some MCI subjects converted at low (negative) SPARE-AD values and others at higher values after years of SPARE-AD increase. However, what was common in most MCI subjects was that they had high rates of SPARE-AD change. In view of the importance of the accurate estimation of rate of SPARE-AD change, future work in our group will emphasize the use of robust image analysis methods for estimation of rate of change. 4D segmentation and warping methods (Shen and Davatzikos, 2004; Xue et al., 2006) which have recently appeared in the literature promise to provide the foundation of future longitudinal analyses.

In Figs 2 and 3, voxel-based comparisons of more Alzheimer's disease-like and CN-like CN individuals demonstrated greater amounts of grey matter in the periventricular regions for the more Alzheimer's disease-like compared with the CN-like group. While more Alzheimer's disease-like CN showed the expected Alzheimer's disease-like patterns of brain atrophy, primarily in the temporal lobe, the increase in estimated grey matter in periventricular regions highlights regions of greater white matter abnormalities. These findings are consistent with a role of increased vascular pathology underlying the progression to Alzheimer's disease. It is important to note that the periventricular white matter signal abnormalities were not used by the classifier in stratifying the subjects, since the classifier constructed from the ADNI Alzheimer's disease and CN individuals (Fan et al., 2008) incorporated only temporal, prefrontal and posterior parietal cortical regions. Therefore, subjects presenting Alzheimer's disease-like atrophy patterns, i.e. more positive SPARE-AD scores, were identified based solely on their cortical atrophy in those regions. The observation that CN in the upper quartile of SPARE-AD scores also showed periventricular leukoareosis suggests that subjects developing Alzheimer's disease-like atrophy

developed vascular pathology in parallel. These findings are consistent with recent evidence that vascular pathology and Alzheimer's disease-type neuropathology act in an additive manner to increase the risk for clinical dementia (Schneider *et al.*, 2004; Troncoso *et al.*, 2008), perhaps by increasing the likelihood that a person will cross the clinical threshold for a diagnosis of dementia. However, concurrent analysis of quantitative measures of progression of vascular disease in combination with measures of atrophy is necessary to better understand whether there might be any causal relationship between these two pathologies, or whether they simply develop in parallel.

Another contribution of the current study is that it evaluates the stability of pattern classification methods across two different large studies, which is important for the clinical applicability and generalization ability of these analysis tools across different clinics as biomarkers of Alzheimer's disease. In particular, the CN and Alzheimer's disease participants of the ADNI study were used to construct a classifier that recognizes Alzheimer's disease-like patterns of brain atrophy (Fan *et al.*, 2008), and was then applied to the BLSA, a completely independent longitudinal study of normal ageing. Previous reports employing similar methods have been restricted to single studies (Davatzikos *et al.*, 2008; Fan *et al.*, 2008; Vemuri *et al.*, 2008) and therefore do not test the generalization ability of these classifiers as biomarkers of Alzheimer's disease. However, recent studies testing similar methods across sites have begun to emerge (Kloppel *et al.*, 2008). These studies suggest that pattern classification methods are likely to be helpful tools in diagnosis of dementia and prognosis of its progression.

One limitation in interpreting our findings is that we do not have a gold standard for evaluation of the meaning of the positive SPARE-AD score, although we hypothesize that increasing spatial atrophy patterns will correspond to increasing Alzheimer's disease pathology. However, our results suggest that future studies should investigate the temporal dynamics of associations between spatial patterns of atrophy, vascular disease, and neuropathology in leading to memory impairment and dementia. Prospective imaging studies, such as the BLSA neuroimaging study, in combination with autopsy assessment of neuropathology will provide important information on the temporal relationships among these cognitive and brain changes in older adults.

Acknowledgements

Funding

References

Benton A. Revised Visual Retention Test. New York: Psychological Corporation; 1974.

Beresford T, Arciniegas D, Alfers J, Clapp L, Martin B, Beresford H, et al. Hypercortisolism in alcohol dependence and its relation to hippocampal volume loss. J Stud Alcohol 2006a; 67: 861–7.

Beresford TP, Arciniegas DB, Alfers J, Clapp L, Martin B, Du Y, et al. Hippocampus volume loss due to chronic heavy drinking. Alcohol Clin Exp Res 2006b; 30: 1866–70.

Blessed G, Tomlinson B, Roth M. The association between quantitative measures of dementia and of senile change in the cerebral grey matter of elderly subjects. Br J Psychiatry 1968; 114: 797–811.

Caffo B, Chen S, Stewart W, Bolla K, Yousem D, Davatzikos C, et al. Are brain volumes based on magnetic resonance imaging mediators of the associations of cumulative lead dose with cognitive function? Am J Epidemiol 2008; 167: 429–37.

Chetelat G, Desgranges B, de la Sayette V, Viader F, Eustache F, Baron J-C. Mapping gray matter loss with voxel-based morphometry in mild cognitive impairment. Neuroreport 2002; 13: 1939–43.

Convit A, de Asis J, de Leon MJ, Tarshish CY, De Santi S, Rusinek H. Atrophy of the medial occipitotemporal, inferior, and middle temporal gyri in non-demented elderly predict decline to Alzheimer's disease. Neurobiol Aging 2000; 21: 19–26.

Convit A, De Leon MJ, Tarshish C, De Santi S, Tsui W, Rusinek H, et al. Specific hippocampal volume reductions in individuals at risk for Alzheimer's disease. Neurobiol Aging 1997; 18: 131–8.

Davatzikos C, Fan Y, Wu X, Shen D, Resnick SM. Detection of prodromal Alzheimer's disease via pattern classification of magnetic resonance imaging. Neurobiol Aging 2008; 29: 514–23.

Davatzikos C, Genc A, Xu D, Resnick SM. Voxel-based morphometry using the RAVENS maps: methods and validation using simulated longitudinal atrophy. NeuroImage 2001; 14: 1361–9.

Davatzikos C, Ruparel K, Fan Y, Shen D, Acharyya M, Loughead J, et al. Classifying spatial patterns of brain activity for lie-detection. Neuroimage 2005a; 28: 663–8.

Davatzikos C, Shen DG, Wu X, Lao Z, Hughett P, Turetsky BI, et al. Whole-brain morphometric study of schizophrenia reveals a spatially complex set of focal abnormalities. JAMA Arch Gen Psychiatry 2005b; 62: 1218–27.

Delis D, Kramer J, Kaplan E, Ober B. California Verbal Learning Test - Research Edition. New York: The Psychological Corporation; 1987.

Driscoll I, Davatzikos C, An Y, Wu X, Shen D, Kraut M, et al. Longitudinal brain changes in cognitively impaired and unimpaired older adults. Presented at Society of Neuroscience, San Diego, CA, 2007.

Duchesne S, Caroli A, Geroldi C, Barillot C, Frisoni GB, Collins DL. MRI-based automated computer classification of probable AD versus normal controls. IEEE Trans Med Imaging 2008; 27: 509–20.

Fan Y, Batmanghelich N, Clark CM, Davatzikos C, the Alzheimer's Disease Neuroimaging Initiative. Spatial patterns of brain atrophy in MCI patients, identified via high-dimensional pattern classification, predict subsequent cognitive decline. Neuroimage 2008; 39: 1731–43.

Fan Y, Rao H, Hurt H, Giannetta J, Korczykowski M, Shera D, et al. Multivariate examination of brain abnormality using both structural and functional MRI. Neuroimage 2007a; 36: 1189–99.

Fan Y, Shen D, Davatzikos C. Classification of structural images via high-dimensional image warping, robust feature extraction, and SVM. In: Duncan JS, Gerig D, editors. MICCAI. Vol. 3749/2005. Palm Springs, California, USA: Springer Berlin/Heidelberg; 2005. p. 1–8.

Fan Y, Shen D, Gur RC, Gur RE, Davatzikos C. COMPARE: Classification of morphological patterns using adaptive regional elements. IEEE Trans Med Imaging 2007b; 26: 93–105.

Folstein M, Folstein S, McHugh P. 'Mini-mental state'. A practical method for grading the cognitive state of patients for the clinician. J Psychiatr Res 1975; 12: 189–93.

Giannakopoulos P, Hof PR, Vallet PG, Giannakopoulos A-S, Charnay Y, Bouras C. Quantitative analysis of neuropathologic changes in the cerebral cortex of centenarians. Prog Neuro-Psychopharmacol Biol Psychiatry 1995; 19: 577–92.

Goldszal AF, Davatzikos C, Pham D, Yan M, Bryan RN, Resnick SM. An image processing protocol for the analysis of MR images from an elderly population. J Comp Assist Tomogr 1998; 22: 827–37.

Golomb J, deLeon MJ, Kluger A, George AE, Tarshish C, Ferris SH. Hippocampal atrophy in normal aging: an association with recent memory impairment. Arch Neurol 1993; 50: 967–73.

Good CD, Scahill RI, Fox NC, Ashburner J, Friston KJ, Chan D, et al. Automatic differentiation of anatomical patterns in the human brain: Validation with studies of degenerative dementias. Neuroimage 2002; 17: 29–46.

Grober E, Hall CB, Lipton RB, Zonderman AB, Resnick SM, Kawas C. Memory impairment, executive dysfunction, and intellectual decline in preclinical Alzheimer's disease. J Int Neuropsychol Soc 2008; 14: 266–78.

Gur R, Davatzikos C, Shen D, Wu X, Fan Y, Hughett P, et al. Whole-brain deformation based morphometry MRI study of schizophrenia. Schizophr Bull 2006; 31: 408.

Kabani N, MacDonald D, Holmes CJ, Evans A. A 3D atlas of the human brain. Neuroimage 1998; 7: S717.

Karas GB, Scheltens P, Rombouts SARB, Visser PJ, Schijndel RAv, Fox NC, et al. Global and local gray matter loss in mild cognitive impairment and Alzheimer's disease. Neuroimage 2004; 23: 708–16.

Kim J-S, Kanaan R, Kaufmann W, Ross C, Calhoun V, Xu D, et al. Abnormal White Matter Organization in Huntington's Disease Evaluated With Diffusion Tensor MRI. Toronto, Canada: ISMRM; 2003.

Kloppel S, Stonnington CM, Chu C, Draganski B, Scahill RI, Rohrer JD, et al. Automatic classification of MR scans in Alzheimer's disease. Brain 2008; 131: 681–9.

Klunk WE, Mathis CA, Price JC, Lopresti BJ, DeKosky ST. Two-year follow-up of amyloid deposition in patients with Alzheimer's disease. Brain 2006; 129: 2805–7.

Lao Z, Shen D, Xue Z, Karacali B, Resnick SM, Davatzikos C. Morphological classification of brains via high-dimensional shape transformations and machine learning methods. Neuroimage 2004; 21: 46–57.

Morris JC. Clinical dementia rating: a reliable and valid diagnostic and staging measure for dementia of the Alzheimer type. Int Psychogeriatr 1997; 9 (Suppl 1): 173–6; discussion 177–8.

Mueller EA, Moore MM, Kerr DC, Sexton G, Camicioli RM, Howieson DB, et al. Brain volume preserved in healthy elderly through the eleventh decade. Neurology 1998; 51: 1555–62.

Mufson EJ, Chen E-Y, Cochran EJ, Beckett LA, Bennett DA, Kordower JH. Entorhinal cortex beta-amyloid load in individuals with mild cognitive impairment. Exp Neurol 1999; 158: 469–90.

Petersen RC, Smith GE, Waring SC, Ivnik RJ, Tangalos EG, Kokmen E. Mild cognitive impairment: clinical characterization and outcome. Arch Neurol 1999; 56: 303–8.

Pham DL, Prince JL. Adaptive fuzzy segmentation of magnetic resonance images. IEEE Trans Med Imaging 1999; 18: 737–52.

Resnick S, Davatzikos C, Kraut M, Zonderman A. Longitudinal changes in MRI volumes in older adults. Neurobiol Aging 2001; 22: 5.

Resnick S, Pham D, Davatzikos C, Kraut M. Sex differences in regional cerebral blood flow: clinical implications for Alzheimer's disease. Neurobiol Aging 2004; 25: 263.

Resnick SM, Goldszal A, Davatzikos C, Golski S, Kraut MA, Metter EJ, et al. One-year age changes in MRI brain volumes in older adults. Cereb Cortex 2000; 10: 464–72.

Resnick SM, Pham DL, Kraut MA, Zonderman AB, Davatzikos C. Longitudinal magnetic resonance imaging studies of older adults: A shrinking brain. J Neurosci 2003; 23: 295–301.

Rowe CC, Ng S, Ackermann U, Gong SJ, Pike K, Savage G, et al. Imaging beta-amyloid burden in aging and dementia. Neurology 2007; 68: 1718–25.

Scheff SW, Price DA, Schmitt FA, Mufson EJ. Hippocampal synaptic loss in early Alzheimer's disease and mild cognitive impairment. Neurobiol Aging 2006; 27: 1372–84.

Schneider JA, Wilson RS, Bienias JL, Evans DA, Bennett DA. Cerebral infarctions and the likelihood of dementia from Alzheimer disease pathology. Neurology 2004; 62: 1148–55.

Shen D, Davatzikos C. HAMMER: hierarchical attribute matching mechanism for elastic registration. IEEE Trans Med Imaging 2002; 21: 1421–39.

Shen D, Davatzikos C. Measuring temporal morphological changes robustly in brain MR images via 4-dimensional template warping. NeuroImage 2004; 21: 1508–17.

Shen DG, Davatzikos C. Very high resolution morphometry using mass-preserving deformations and HAMMER elastic registration. Neuroimage 2003; 18: 28–41.

Stewart WF, Schwartz BS, Davatzikos C, Shen D, Liu D, Wu X, et al. Past adult lead exposure is linked to neurodegeneration measured by brain MRI. Neurology 2006; 66: 1476–84.

Sullivan EV, Pfefferbaum A, Adalsteinsson E, Swan GE, Carmelli D. Differential rates of regional brain change in callosal and ventricular size: a 4-year longitudinal MRI study of elderly men. Cereb Cortex 2002; 12: 438–45.

Troncoso JC, Zonderman AB, Resnick SM, Crain B, Pletnikova O, O'Brien RJ. Effect of infarcts on dementia in the Baltimore longitudinal study of aging. Ann Neurol 2008; 64: 168–176.

Vemuri P, Gunter JL, Senjem ML, Whitwell JL, Kantarci K, Knopman DS, et al. Alzheimer's disease diagnosis in individual subjects using structural MR images: Validation studies. Neuroimage 2008; 39: 1186–97.

Xue Z, Shen D, Davatzikos C. CLASSIC: Consistent longitudinal alignment and segmentation for serial image computing. Neuroimage 2006; 30: 388–99.

Ziolko SK, Weissfeld LA, Klunk WE, Mathis CA, Hoge JA, Lopresti BJ, et al. Evaluation of voxel-based methods for the statistical analysis of PIB PET amyloid imaging studies in Alzheimer's disease. Neuroimage 2006; 33: 94–102.